RSC Advances

PAPER

View Article Online
View Journal | View Issue

Cite this: *RSC Adv.*, 2020, **10**, 14595

Functionalization and antioxidant activity of polyaniline–fullerene hybrid nanomaterials: a theoretical investigation†

Nguyen Minh Thong,[a] Quan V. Vo,[b] Trinh Le Huyen,[cd] Mai Van Bay,[e] Nguyen Nho Dung,[f] Pham Thi Thu Thao[dg] and Pham Cam Nam[d]

Received 30th January 2020
Accepted 23rd March 2020

DOI: 10.1039/d0ra00903b

rsc.li/rsc-advances

Functionalized fullerene is one of the most advantageous nanotechnologies to develop novel materials for potential biomedical applications. In this study, we applied the ONIOM-GD3 approach to explore the nucleophilic addition reaction mechanism between polyaniline (emeraldine and leucoemeraldine forms) and fullerene. Potential energy surfaces were also analyzed to predict the predominantly formed products of the functionalized reaction. The themoparameters, such as bond dissociation enthalpy (BDE), ionization energy (IE), and electron affinity (EA), characterized by two mechanisms HAT and SET, were used to evaluate the antioxidant activities of the selected compounds. Moreover, the calculated HOMO, LUMO, and DOS results indicate that the electronic structures of polyaniline–fullerene were significantly affected by the presence of fullerene. The computational results show that **C60-L1** seems to be the best antioxidant following the SET mechanism.

1. Introduction

Nowadays, hybrid nanomaterials formed between conjugated polymers and carbon nanomaterials have been attracting considerable attention from experimental and theoretical researchers because of their important role in developing science and technologies.[1–4]

Polyaniline belong to the family of π-conjugated polymers and its low cost as well as high application potential has attracted significant attention. Recently, the antioxidant activity of polyaniline has attracted substantial interest in biomedical applications. Polyaniline can be combined with carbon nanomaterials such as fullerenes,[5,6] carbon nanotubes,[7] and graphene.[8,9] Among them, [60]fullerene has raised much interest in the field of biomedical applications and materials science[10–14] due to their attractive chemical–physical characteristics. In fact, fullerene has been regarded as 'radical sponges' to trap multiple radicals per molecule.[15,16] Functionalization of fullerene is well known as a worthy way to develop the new fullerene based nanomaterials. In fact, the nucleophilic addition reactions between aromatic amines and fullerene by using solvent-free gas phase have been one of the most widely used functionalization approaches because this technique helps to prevent the contamination by impurities and organic solvents, which is important for biomedical applications.[17]

For the large molecular systems such as fullerene derivatives, in order to determine accurately the reaction mechanism of fullerene functionalization, the ONIOM method developed by Morokuma and coworkers is one of the suitable choices.[18] In fact, numerous previous studies applied the two-layered ONIOM approach for the investigation of chemical reactions involving fullerene.[19–22] To get an accurate description of the energy profile for the study of the reaction of fullerene functionalization,[21] the GD3 empirical dispersion correction, according to Grimme,[23] was also taken into account in the ONIOM approach (ONIOM-GD3).

Based on the experimental reaction,[17] the reaction mechanism between aniline and fullerene (Fig. 1) was reproduced and studied in detail *via* the ONIOM-GD3 method. Then, we systematically explored the possible reaction paths for fullerene functionalization based on the reactions of polyaniline in the

[a]*The University of Danang, Campus in Kon Tum, 704 Phan Dinh Phung, Kon Tum 580000, Vietnam. E-mail: nmthong@kontum.udn.vn*

[b]*The University of Danang, University of Technology and Education, 48 Cao Thang, Danang 550000, Vietnam. E-mail: vvquan@ute.udn.vn*

[c]*Department of Applied Chemistry, National Chiao Tung University, Hsinchu 30010, Taiwan*

[d]*Department of Chemical Engineering, The University of Danang, University of Science and Technology, 54 Nguyen Luong Bang, Danang 550000, Vietnam. E-mail: pcnam@dut.udn.vn*

[e]*The University of Danang, University of Science and Education, Danang 550000, Vietnam*

[f]*Danang University of Physical Education and Sports, Danang 550000, Vietnam*

[g]*Department of Chemistry, University of Sciences, Hue University, 77 Nguyen Hue, Hue 530000, Vietnam*

† Electronic supplementary information (ESI) available. See DOI: 10.1039/d0ra00903b

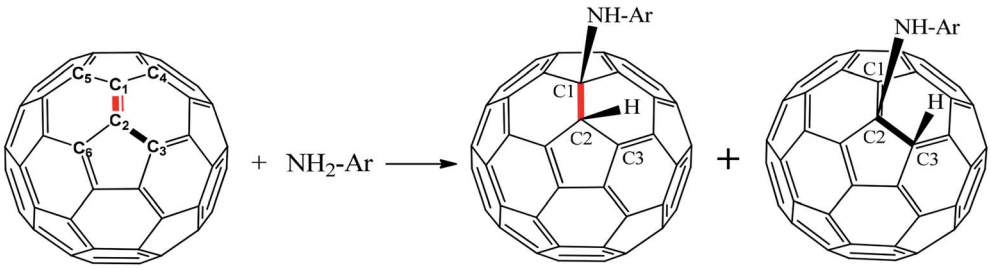

Fig. 1 Possible product in the reaction between [60]fullerene and aniline.

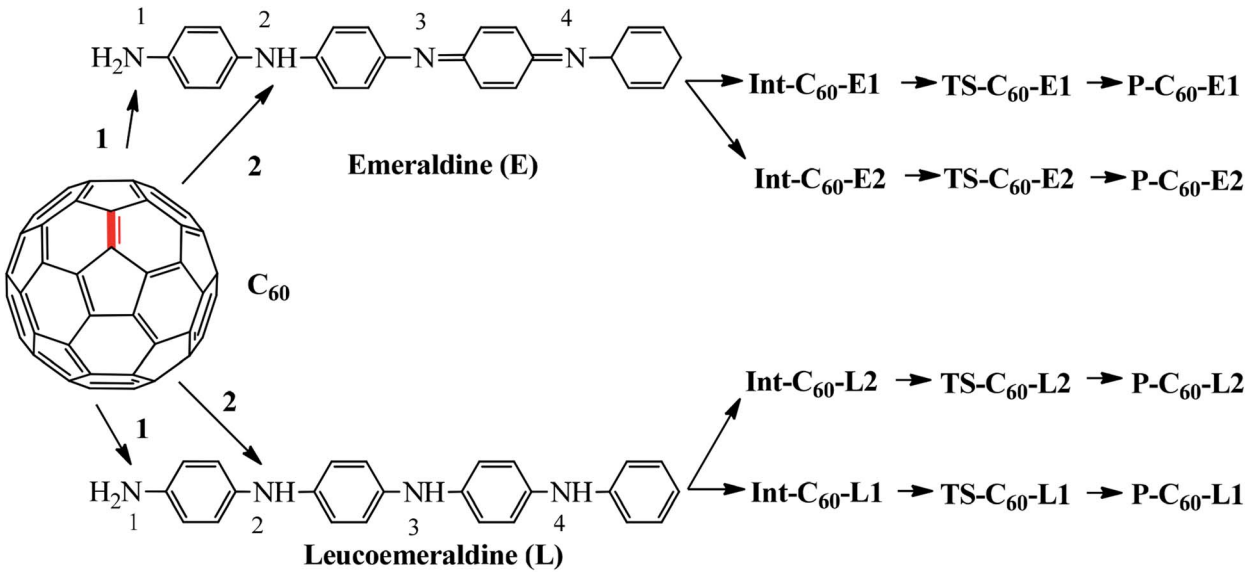

Fig. 2 Possible reaction paths between [60]fullerene with emeraldine and leucoemeraldine.

form of emeraldine (E) and leucoemeraldine (L) using the same ONIOM-GD3 method (Fig. 2). A question was raised about what kind of these products is preferably formed. To solve this problem, the potential energy surface (PES) was investigated to clarify the mechanism of these reactions.

To date, numerous studies on antioxidant activity of polyaniline[24,25] and fullerene[26] have been reported. For aromatic amine antioxidants, the reaction mechanism and rate depend on the hydrogen atom's donating ability to peroxyl radicals. Moreover, the characteristics of fullerenes have an extended π-bond system, and their electron affinity is higher than that of primary antioxidants. Thus, the question is whether the derivatization of fullerenes with polyaniline is expected to increase their antioxidant capacity. However, theoretical approaches on the radical scavenging activity of new polyaniline–fullerene have not been realized in the literature yet. Therefore, we aim to predict the antioxidant activities of polyaniline–fullerene *via* single electron transfer (SET) and hydrogen atom transfer (HAT) mechanisms along with the important thermal-parameters such as ionization energy (IE), electron affinity (EA), and bond dissociation enthalpy (BDE) parameters.

In this study, we focus on studying the mechanism for the reaction of fullerene with the two forms of polyaniline as well as to evaluate the antioxidant ability of polyaniline–fullerene hybrid nanomaterials using the ONIOM-GD3 (B3LYP/6-31G(d):PM6) and hybrid density functional theory (DFT) methods.

2. Computational methods

All the electronic structures of species involved in the title reaction as reactants, intermediates, transition states, and products were optimized using the two-layered ONIOM-GD3 (B3LYP/6-31G(d):PM6) method including Grimme's dispersion corrections.[23] The transition states were first obtained and then confirmed by the presence of one imaginary frequency. Furthermore, the intrinsic reaction coordinate (IRC) was also performed for analyzing the connection between the transition states (TS) and two related local minimum structures.

The geometry and the vibrational frequency of the composited polyaniline–fullerene and the related neutral, cationic, and anionic radicals were carried out at the B3LYP/6-31G(d) method.[27,28] From these optimized structures, the single-point

energy calculations were employed at the level of B3LYP/6-311++G(d,p).

Moreover, the full-electron donor–acceptor map (FEDAM) was established to analyze the radical scavenging activity of the studied compounds *via* the electron acceptance (REA) and electron donation (RIE) indices, which were defined according to the equations:

$$\mathrm{RIE} = \frac{\mathrm{IE_{Anti}}}{\mathrm{IE_{Na}}}$$

$$\mathrm{REA} = \frac{\mathrm{EA_{Anti}}}{\mathrm{EA_{F}}}$$

where Anti, Na, and F represent the antioxidant molecule, sodium, and *fluorum*, respectively.

The calculations for this study were performed using the Gaussian 09 software.[29]

3. Results and discussion

3.1. Functionalized fullerene using the ONIOM method

First, the reliability of the model of fullerene and aniline using the ONIOM-GD3 (B3LYP/6-31G(d):PM6) method in this study was tested by comparing the optimized structures and thermodynamic parameters of reactants, transition states, and products with the computed values using B3LYP-GD3/6-31+G(d) for all atoms in this system. The results are shown in Table 1. For convenience, the intermediates, transition states, and products are marked as "**Int**", "**TS**", and "**P**" acronyms, respectively.

As can be seen in Table 1, the optimized bond distances of fullerene using the ONIOM-GD3 (B3LYP/6-31G(d):PM6) method agree well with the experimental data. Indeed, the calculated/experimental [5-6] (C2–C3) and [6-6] (C1–C2) bonds were 1.458/1.458 Å and 1.401/1.401 Å, respectively.[30] The calculated data at the ONIOM-GD3 (B3LYP/6-31G(d):PM6) and B3LYP-GD3/6-31+G(d) levels of theory in Table 1 show that the geometrical parameters of the transition states and products have a very small deviation in the range of −0.028 to 0.028 Å. For the thermodynamic parameters, the deviation between the two methods is in the range of 0.9 to 5.3 kcal mol^{-1}. It can be observed that the calculated values obtained in the proposed ONIOM-GD3 model were in very good agreement with the corresponding data obtained using the B3LYP-GD3/6-31+G(d) method for the whole system. Thus, this ONIOM-GD3 partition is recommended as a reliable and computationally affordable approach to be exploited in this study.

In the initial step, the association of fullerene and aniline formed an intermediate (**Int**) with a binding energy of −4.0 kcal mol^{-1} lower than the reactants (see Fig. 3). This

Table 1 The optimized structures and thermodynamic parameters of all species related to the reaction of aniline and fullerene in the gas phase

Species		ONIOM-GD3 (B3LYP/6-31G(d):PM6)	B3LYP-GD3/6-31+G(d)	Deviation[c]
Optimized structures (bond distance)[a]				
Fullerene	C1–C2	1.401	1.396 (1.401)[d]	−0.005 (0.000)
	C2–C3	1.458	1.454 (1.458)[d]	−0.004 (0.000)
TS(5,6)	C1–C2	1.486	1.483	−0.003
	C2–C3	1.610	1.582	−0.028
	C2–C6	1.529	1.525	−0.004
	C2–N	1.580	1.608	0.028
TS(6,6)	C1–C2	1.574	1.555	−0.019
	C1–C4	1.523	1.521	−0.002
	C1–C5	1.525	1.523	−0.002
	C1–N	1.582	1.590	0.008
P(5,6)	C1–C2	1.537	1.527	−0.010
	C2–C3	1.640	1.624	−0.016
	C2–C6	1.547	1.543	−0.004
	C2–N	1.467	1.473	0.006
P(6,6)	C1–C2	1.627	1.601	−0.026
	C1–C5	1.544	1.544	0.000
	C1–C4	1.556	1.553	−0.003
	C1–N	1.465	1.472	0.007
Relative energies[b]				
	Reactants	0.0	0.0	0.0
	Int	−4.0	−3.1	0.9
	TS(5,6)	44.1	48.4	4.3
	TS(6,6)	32.8	36.4	3.6
	P(5,6)	9.9	15.2	5.3
	P(6,6)	−4.9	−2.4	2.5

[a] Distance is in angstroms Å. [b] Relative energy in kcal mol^{-1} (zero-point energies were included). [c] Values (B3LYP-GD3/6-31+G(d)) – values (ONIOM-GD3 (B3LYP/6-31G(d):PM6)). [d] Ref. 30.

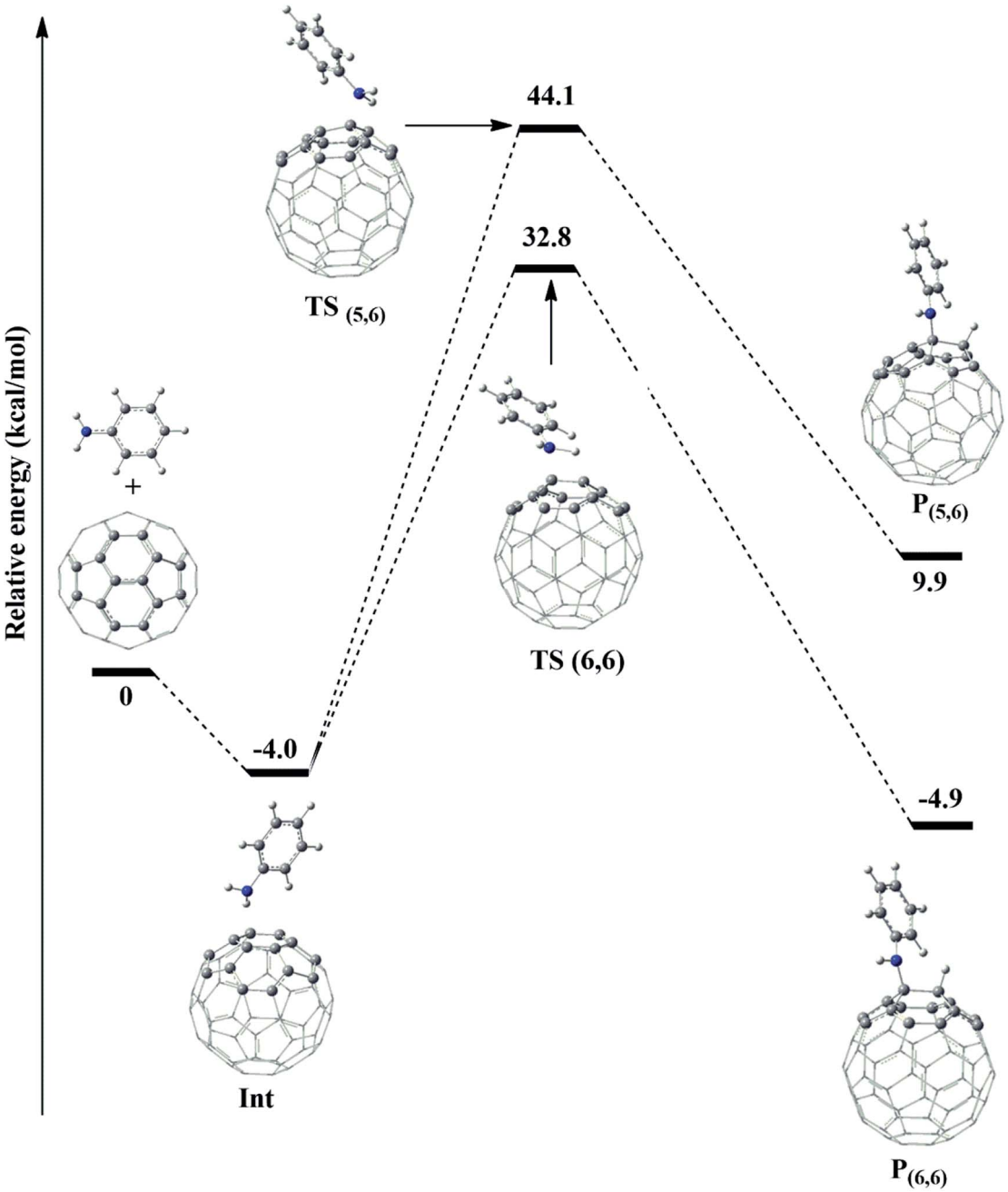

Fig. 3 PES of the functionalized reaction between fullerene and aniline.

intermediate can proceed through two channels for the abstraction process of fullerene. The first one was a process at the (6,6)–bond to yield **TS(6,6)**, whose energy barrier was 36.8 kcal mol^{-1}. The second one occurs to form **P(5,6)** at the (5,6)–bond *via* the transition state **TS(5,6)** during the reaction, as confirmed by one imaginary vibrational frequency and IRC analysis presented in Table S1 and Fig. S1 of ESI.† As shown in Fig. 3, the energy barrier of **TS(5,6)** was higher than that of **TS(6,6)** by 11.3 kcal mol^{-1}. Therefore, a conclusion can be drawn that the process for the **P(6,6)** product was energetically favored than that for **P(5,6)** product. It is clear that the theoretical results obtained from this section are also similar to the experimental procedures in order to synthesize aniline–fullerene.[17]

Thus, the PES of the reaction between fullerene and polyaniline (**PANI**) focus only on the (6-6)–bond, which is illustrated in Fig. 3. Depending on the environment, the structure of **PANI** consists of three forms, including leucoemeraldine (**PANI-L**), pernigraniline (**PANI-P**), and emeraldine (**PANI-E**). However, in this context, we chose two forms, namely **PANI-L** and **PANI-E**, to investigate the functionalized reaction of fullerene with

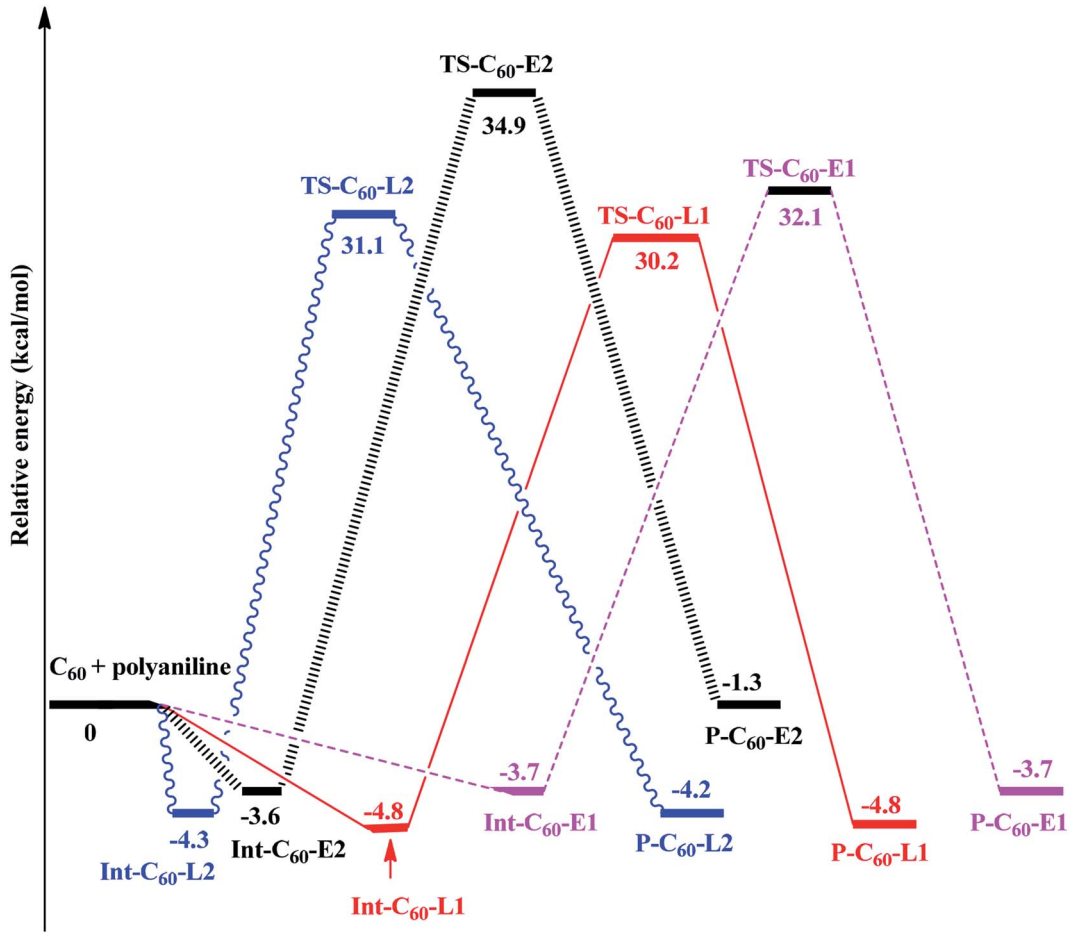

Fig. 4 PES of the functionalized reaction between fullerene and two forms of polyaniline.

polyaniline because the structure of pernigraniline does not possess the –NH group to perform the amination reaction.

Fig. 4 shows that all the obtained reactions of two forms of polyaniline with fullerene have tended to be quite similar. Energies of all the species and energy barriers for the reaction between fullerene and two forms of polyaniline using the ONIOM-GD3 (B3LYP/6-31G(d):PM6) method are summarized in Tables S1 and S2 (ESI†). The intermediates being a local minimum on the potential energy surface were formed from the reactants, without transition states. The relative energies to the corresponding intermediates **Int-C$_{60}$-E1**, **Int-C$_{60}$-E2**, **Int-C$_{60}$-L1**, and **Int-C$_{60}$-L2** were −3.7, −3.6,−4.8, and −4.3 kcal mol^{-1}, respectively. The reaction pathway diagram shows that the energy barriers of **TS-C$_{60}$-E1**, **TS-C$_{60}$-E2**, **TS-C$_{60}$-L1**, and **TS-C$_{60}$-L2** were 35.8, 38.5, 35.0, and 35.4 kcal mol^{-1}, respectively. The relative energies of products, namely **P-C$_{60}$-E1**, **P-C$_{60}$-E2**, **P-C$_{60}$-L1**, and **P-C$_{60}$-L2**, were predicted to be −3.7, −1.3, −4.8, and −4.2 kcal mol^{-1}, respectively, in comparison to the reactants. Thus, this obtained result suggests that **P-C$_{60}$-E1**, **P-C$_{60}$-L1**, and **P-C$_{60}$-L2** products were predominantly formed from a thermodynamic point of view.

3.2. Antioxidant mechanisms

The structure of polyaniline–fullerene consists of two typical segments: polyaniline known as chain-breaking antioxidants[25,31] and fullerene known as an extended π-bond system and a high electron affinity.[32] For this reason, both HAT and SET mechanisms were used to analyze the radical quenching capacity of the products of reactions between fullerene and the two forms of polyaniline. The structures of **C60-L1**, **C60-L2**, **C60-E1**, and **C60-E2** are shown in Fig. 5. The thermochemical parameters characterized by antioxidant activity (BDE, IE, and EA) were calculated using the B3LYP/6-311++G(d,p)//B3LYP/6-31G(d) model. Moreover, the Grimme's dispersion corrections[23] were included to evaluate the effects of dispersion interactions on the thermochemical parameters. As can be seen in Tables S3 and S4 (ESI†), the deviation between BDE, IE, and EA calculated at the B3LYP-GD3 and B3LYP levels were very small (<1.0 kcal mol^{-1}). Therefore, the effects of dispersion interactions on the thermochemical parameters are insignificant.

Hydrogen atom transfer mechanisms (HAT). The free radical scavenging activity *via* the H-atom transfer mechanism was mainly characterized by the BDE value. In amine compounds, the N–H bond dissociation enthalpy (hydrogen abstraction) is the key parameter to evaluate the abilities to donate hydrogen

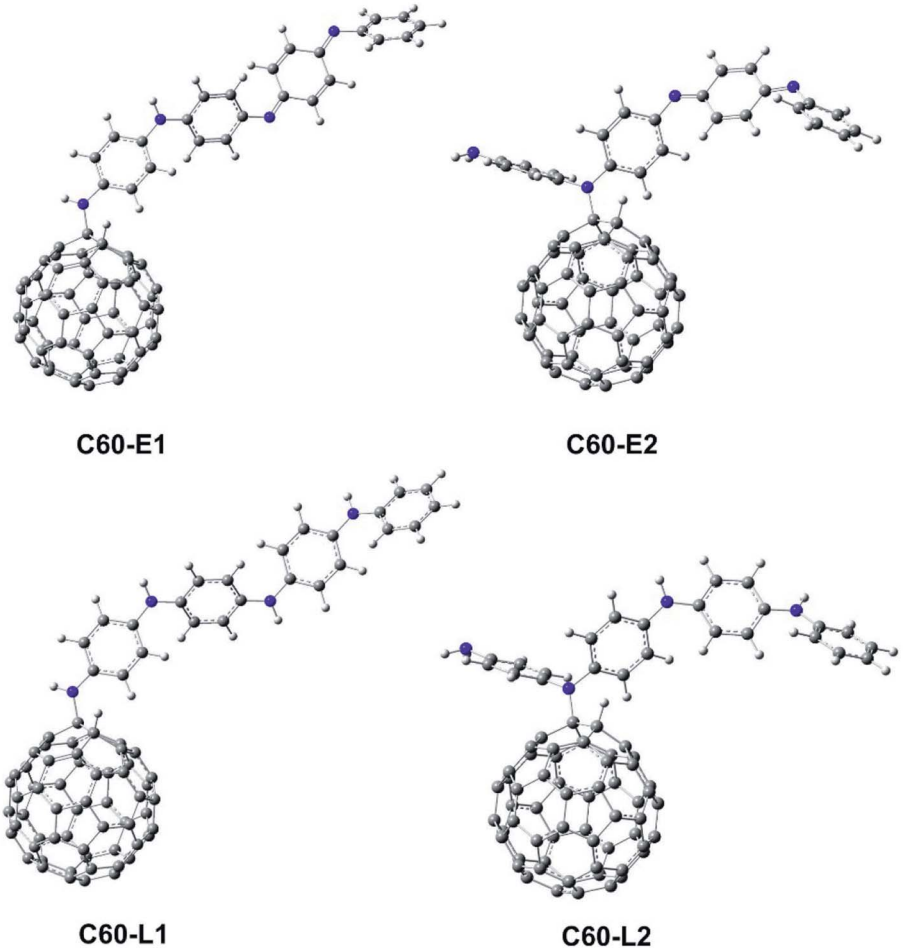

Fig. 5 The structures of C60-L1, C60-L2, C60-E1, and C60-E2.

atom and form a stable radical form. The molecules with lower BDE values had higher antioxidant activity. As can be seen in Table 2 that the difference of BDE(N–H)s between the polyanilines (**PANI-L**, **PANI-E**) and the polyaniline–fullerene hybrid nanomaterials (**C60-L1**, **C60-L2**, **C60-E1**) was insignificant (<2 kcal mol^{-1}). This result leads to a suggestion that the antioxidant activity of the hybrid materials following the HAT mechanism may not be higher than that of the polyanilines. Thus, the effects of the fullerene on the BDE(N–H)s as well as the hydrogen abstraction of **PANI-L** or **PANI-E** have been unnoticeable.

Table 2 Calculated BDE(N–H) at B3LYP/6-311++G(d,p)//B3LYP/6-31G(d) level of theory

Compounds	BDE(N–H) (kcal mol^{-1})	Compounds	BDE(N–H) (kcal mol^{-1})
PANI-L		**C60-L2**	
N1–H	85.09	N1–H	89.78
N2–H	78.04	N3–H	79.75
N3–H	78.10	N4–H	81.14
N4–H	79.92		
PANI-E		**C60-E1**	
N1–H	86.83	N1–H	83.86
N2–H	78.66	N2–H	78.93
C60-L1		**C60-E2**	
N1–H	81.85	N1–H	90.88
N2–H	78.14		
N3–H	78.31		
N4–H	80.21		

Table 3 Calculated IE and EA at B3LYP/6-311++G(d,p)//B3LYP/6-31G(d) level of theory

Compounds	Adiabatic IE (kcal mol^{-1})	Adiabatic EA (kcal mol^{-1})
PANI-L	130.36	0.58
PANI-E	140.74	45.62
C60-L1	130.98	65.10
C60-L2	133.97	61.74
C60-E1	140.56	66.46
C60-E2	143.84	65.18

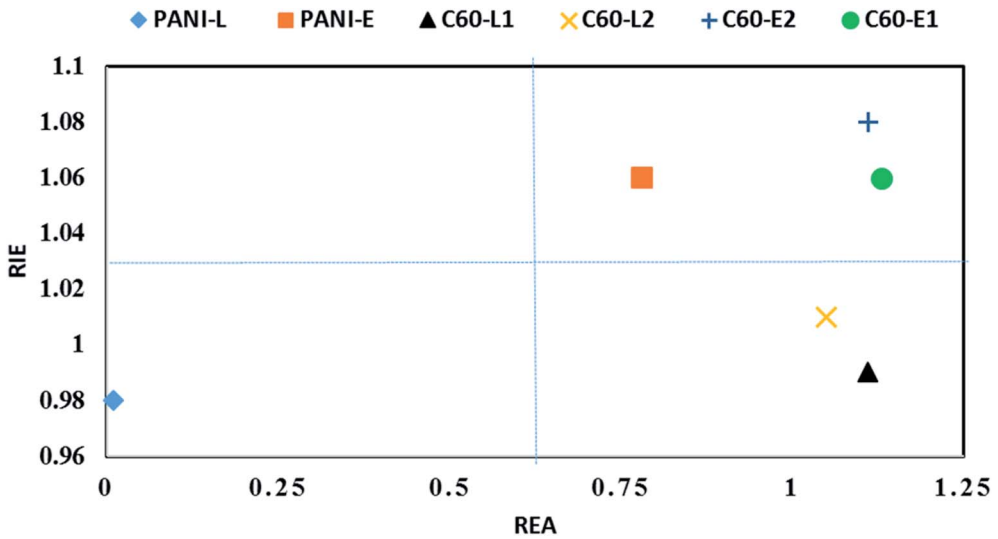

Fig. 6 FEDAM of the studied compound in the gas phase.

Single electron transfer (SET). The electron transfer mechanism (SET) involves an electron-donating/-accepting process. Thus, when evaluating the antioxidant activity of the selected compounds according to the SET mechanism, we have investigated based on both their electron-donor and electron-acceptor capacities, which are characterized by the ionization energy (IE) and electron affinity (EA) quantity.[33] It is generally observed that the lower the IE value, the easier the electron transfer, and the higher the EA value represents the stronger electron acceptor capacity. In this study, the IEs and EAs were calculated in adiabatic states using the same calculating method and are presented in Table 3.

It was found that the IE values of the materials (130.98–143.84 kcal mol^{-1}) were larger than those of the polyanilines (130.36–140.74 kcal mol^{-1}). This suggests that the polyaniline–fullerene hybrid nanomaterials hardly transferred an electron compared with the initial polyanilines. However, it is worth noticing that the EAs of the materials were significantly higher than those of the polyanilines (averaged about 29.83 kcal mol^{-1}). Thus, the accepting-electron process seems to be the main mechanism responsible for the antioxidant activity of the polyaniline–fullerenes.

Based on FEDAM shown in Fig. 6, it can be seen that **C60-L1** belongs to the best antioxidant sector. It demonstrates that **C60-L1** simultaneously plays the two roles as a good electron donator and a good electron acceptor.

Frontier molecular orbitals. The frontier orbital distributions and energies calculated in the gas phase at the level of B3LYP/6-311++G(d,p)//B3LYP/6-31G(d) are shown in Fig. 7, and density of state (DOS) spectra are also indicated in Fig. 8. These are also important parameters as they correlate with the antioxidative activity of the studied compounds. The highest occupied molecular orbital (HOMO) of the polyaniline–fullerene is mainly distributed in polyaniline, while the lowest unoccupied molecular orbital (LUMO) is allocated in fullerene (Fig. 7). According to the frontier orbital theory, the energy of the HOMO and LUMO provides a quantitative measure of the electron-donating and accepting ability of the antioxidants. The higher energy of the HOMO corresponds with an easier electron-donating ability. On the contrary, the lower energy of the LUMO corresponds to a stronger electron accepting abilities. As shown in Fig. 6, the HOMO energy increases in the following order: **C60-E2** < **C60-E1** < **PANI-E** < **C60-L2** < **C60-L1** < **PANI-L**, while the LUMO energy decreases in the following order: **PANI-L** > **PANI-E** > **C60-L2** > **C60-L1** > **C60-E2** > **C60-E1**. By comparison, according to HOMO and LUMO energies, the predicted electron-donating and accepting ability sequence was found to be the same as that for the IE and EA. Another important parameter of the investigated compounds is the HOMO–LUMO energy gaps (E_{gap}). The lower the E_{gap}, the easier the electron inspires, and the more powerful is the antioxidant ability.[34] The different energy of E_{gap} in polyaniline–fullerene hybrid nanomaterials is nicely demonstrated in the DOS spectra (Fig. 8). It clearly shows that **C60-L** has the strongest antioxidant ability among the selected compounds.

3.3. Reaction between $CH_3OO^{\bullet}$, $O_2^{\bullet -}$ and polyaniline–fullerene

The interaction between polyaniline–fullerene and $CH_3OO^{\bullet}$ and $O_2^{\bullet -}$ was evaluated through an electron transfer mechanism in the gas phase to provide more insight into their free radical quenching capacity following the reaction equations:

$$\text{Anti} + R^{\bullet} \rightarrow \text{Anti}^{+\bullet} + R^{-} \quad (1)$$

$$\text{Anti} + R^{\bullet} \rightarrow \text{Anti}^{-\bullet} + R^{+} \quad (2)$$

As can be seen in Table 4, the reactions Anti + $CH_3OO^{\bullet}$ following (1) and (2) are unspontaneous with the high positive thermal barriers of ΔH and ΔG ($\Delta H = 111.2 \div 266.6$ kcal mol^{-1}, $\Delta G = 114.7 \div 265.6$ kcal mol^{-1}). The trend was similar in the

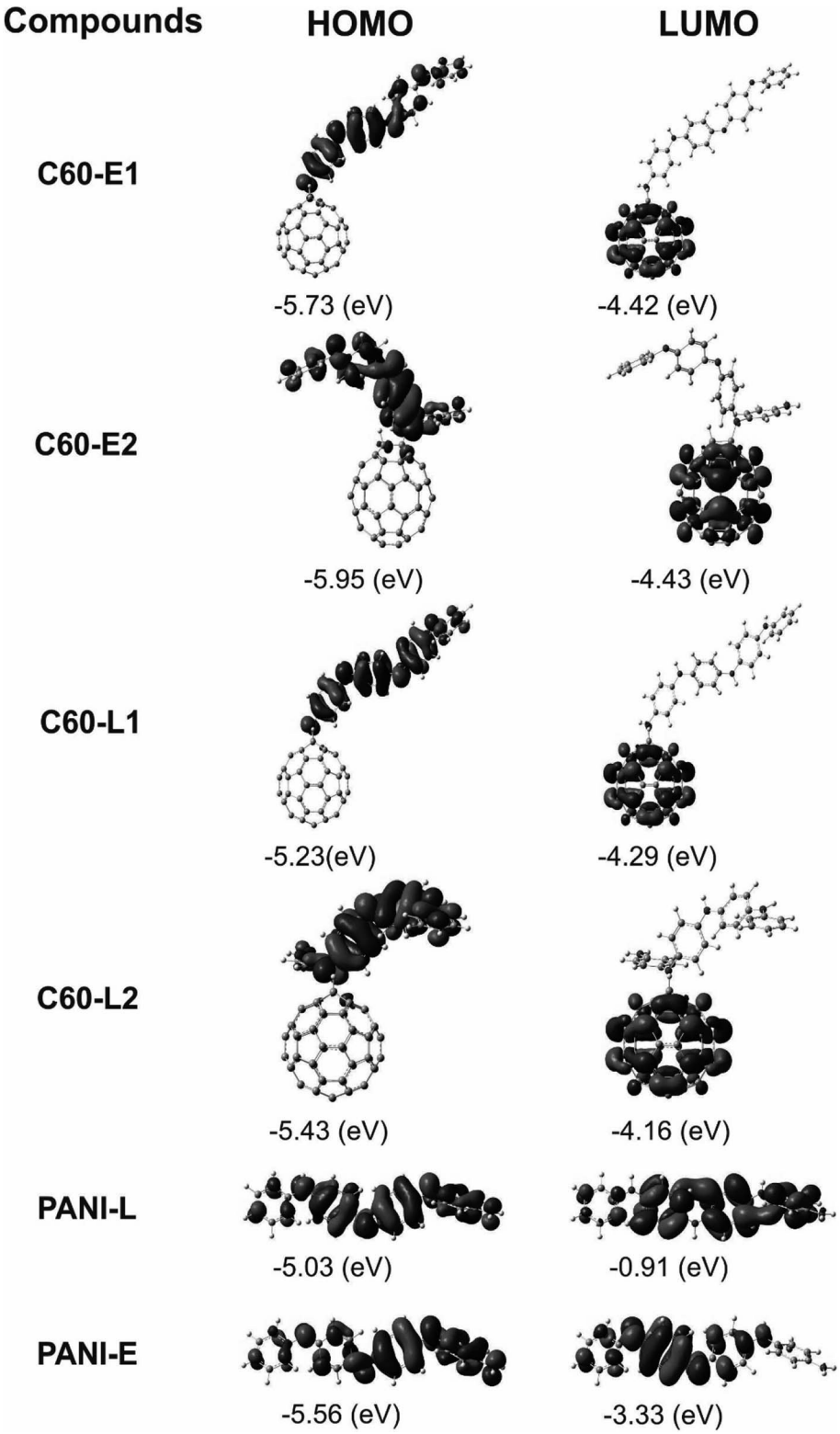

Fig. 7 The HOMO, LUMO distributions and energies of the studied compound.

electron-donating process of the Anti + $O_2^{\bullet -}$ reaction. However, it is worth noticing that the electron-accepting process of the Anti + $O_2^{\bullet -}$ reaction following (2) was spontaneous ($\Delta H = -15.2 \div -20.8$ kcal mol^{-1}, $\Delta G = -16.7 \div -20.7$ kcal mol^{-1}), whereas that for the initial polymers was unspontaneous ($\Delta G > 0$). This affirms that the polyaniline–fullerene materials are good in $O_2^{\bullet -}$ scavenging following the electron-accepting mechanism. This is a good agreement with the previous studies.[35]

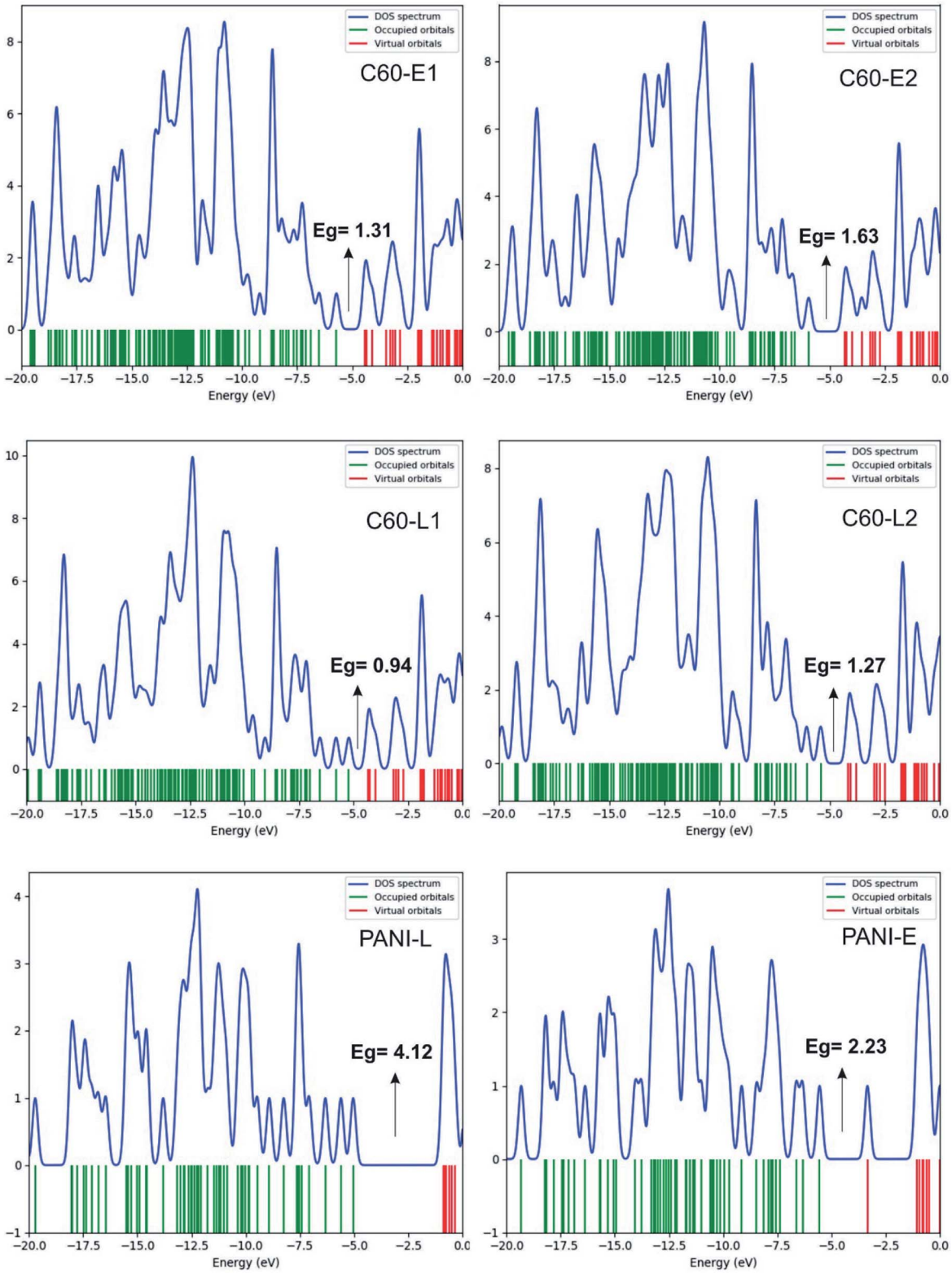

Fig. 8 DOS spectra of fullerene, polyaniline and polyaniline–fullerene hybrid nanomaterials.

Table 4 The calculated thermal properties (in kcal mol^{-1}) of the reaction between $CH_3OO^{\bullet}$, $O_2^{\bullet -}$and polyaniline–fullerene

	Anti + $CH_3OO^{\bullet}$				Anti + $O_2^{\bullet -}$			
	Reaction (1)		Reaction (2)		Reaction (1)		Reaction (2)	
Compounds	ΔH	ΔG	ΔH	ΔG	ΔH	ΔG	ΔH	ΔG
C60-L1	113.4	114.7	190.1	190.3	339.9	340.6	−19.0	−18.9
C60-L2	115.7	117.3	193.9	192.5	342.2	343.2	−15.2	−16.7
C60-E1	123.6	124.6	188.3	188.5	350.0	350.5	−20.8	−20.7
C60-E2	126.4	127.8	190.3	190.4	352.8	353.7	−18.8	−18.8
PANI-L	111.2	113.0	266.6	265.6	337.6	338.9	57.5	56.4
PANI-E	122.1	123.2	213.8	212.9	348.6	349.1	4.7	3.7

4. Conclusion

In this study, some conclusions in investigating the characteristics of new polyaniline–fullerene materials can be drawn as:

- Potential energy surfaces of the reaction between fullerene and polyaniline (PANI) were analyzed *via* the ONIOM method. The obtained result suggests that **P-C_{60}-E1**and **P-C_{60}-L1** products were predominantly formed.

- Evaluating the antioxidant activity of polyaniline–fullerene materials using these themoparameters (BDE, IE, and EA) established the HAT and SET mechanism and found that the favored mechanism is the electron-accepting one. In addition to the calculated HOMO, LUMO, DOS, and FEDAM results show that **C60-L** has the strongest antioxidant activity among the new polyaniline–fullerene materials.

Conflicts of interest

There are no conflicts to declare.

Acknowledgements

This research is funded by Vietnam National Foundation for Science and Technology Development (NAFOSTED) under grant number 104.06-2018.42.

References

1 S. Xiong, F. Yang, H. Jiang, J. Ma and X. Lu, Covalently bonded polyaniline/fullerene hybrids with coral-like morphology for high-performance supercapacitor, *Electrochim. Acta*, 2012, **85**, 235–242, DOI: 10.1016/j.electacta.2012.08.056.

2 S. Xiong, *et al.*, Covalent bonding of polyaniline on fullerene: Enhanced electrical, ionic conductivities and electrochromic performances, *Electrochim. Acta*, 2012, **67**, 194–200, DOI: 10.1016/j.electacta.2012.02.026.

3 H. Wang, X. Yan and G. Piao, A high-performance supercapacitor based on fullerene C 60 whisker and polyaniline emeraldine base composite, *Electrochim. Acta*, 2017, **231**, 264–271, DOI: 10.1016/j.electacta.2017.02.057.

4 N. Politakos, I. Zalakain, B. Fernandez d'Arlas, A. Eceiza and G. Kortaberria, Optical, structural and electrical properties of polyaniline systems doped with C60 and small gap C60 fullerenes, *Mater. Chem. Phys.*, 2013, **142**, 387–394, DOI: 10.1016/j.matchemphys.2013.07.033.

5 M. Gizdavic-Nikolaidis, J. Vella, G. A. Bowmaker and Z. D. Zujovic, Rapid microwave synthesis of polyaniline–C 60 nanocomposites, *Synth. Met.*, 2016, **217**, 14–18, DOI: 10.1016/j.synthmet.2016.03.009.

6 I. Y. Sapurina, *et al.*, Polyaniline composites with fullerene C60, *Phys. Solid State*, 2002, **44**, 574–575, DOI: 10.1134/1.1462712.

7 M. Baibarac, I. Baltog, S. Lefrant, J. Y. Mevellec and O. Chauvet, Polyaniline and Carbon Nanotubes Based Composites Containing Whole Units and Fragments of Nanotubes, *Chem. Mater.*, 2003, **15**, 4149–4156, DOI: 10.1021/cm021287x.

8 L. Feng, *et al.*, Structure stability of polyaniline/graphene nanocomposites in gamma-ray environment, *J. Radioanal. Nucl. Chem.*, 2018, **315**, 627–638, DOI: 10.1007/s10967-018-5710-y.

9 G. Wang, W. Xing and S. Zhuo, The production of polyaniline/graphene hybrids for use as a counter electrode in dye-sensitized solar cells, *Electrochim. Acta*, 2012, **66**, 151–157, DOI: 10.1016/j.electacta.2012.01.088.

10 X. Zhang, H. Cong, B. Yu and Q. Chen, Recent Advances of Water-Soluble Fullerene Derivatives in Biomedical Applications, *Mini-Rev. Org. Chem.*, 2018, **16**, 92–99, DOI: 10.2174/1570193x15666180712114405.

11 M. Mohajeri, B. Behnam and A. Sahebkar, Biomedical applications of carbon nanomaterials: Drug and gene delivery potentials, *J. Cell. Physiol.*, 2018, **234**, 298–319, DOI: 10.1002/jcp.26899.

12 F. Moussa, [60]Fullerene and derivatives for biomedical applications, 113–136, 2018, DOI: 10.1016/b978-0-08-100716-7.00005-2.

13 S. Goodarzi, T. Da Ros, J. Conde, F. Sefat and M. Mozafari, Fullerene: biomedical engineers get to revisit an old friend, *Mater. Today*, 2017, **20**, 460–480, DOI: 10.1016/j.mattod.2017.03.017.

14 X. Zhu, M. Sollogoub and Y. Zhang, Biological applications of hydrophilic C60 derivatives (hC60s)- a structural

perspective, *Eur. J. Med. Chem.*, 2016, **115**, 438–452, DOI: 10.1016/j.ejmech.2016.03.024.

15 P. J. Krusic, E. Wasserman, P. N. Keizer, J. R. Morton and K. F. Preston, Radical reactions of c60, *Science*, 1991, **254**, 1183–1185, DOI: 10.1126/science.254.5035.1183.

16 J. R. Morton, F. Negri and K. F. Preston, Addition of Free Radicals to C60, *Acc. Chem. Res.*, 1998, **31**, 63–69, DOI: 10.1021/ar950120p.

17 I. J. Ramírez-Calera, *et al.*, Solvent-free functionalization of fullerene C60 and pristine multi-walled carbon nanotubes with aromatic amines, *Appl. Surf. Sci.*, 2015, **328**, 45–62, DOI: 10.1016/j.apsusc.2014.11.188.

18 L. W. Chung, *et al.*, The ONIOM Method and Its Applications, *Chem. Rev.*, 2015, **115**, 5678–5796, DOI: 10.1021/cr5004419.

19 S. Osuna, J. Morera, M. Cases, K. Morokuma and M. Sola, Diels-Alder reaction between cyclopentadiene and C60: an analysis of the performance of the ONIOM method for the study of chemical reactivity in fullerenes and nanotubes, *J. Phys. Chem. A*, 2009, **113**, 9721–9726, DOI: 10.1021/jp904294y.

20 S. Filippone, *et al.*, On the mechanism of the thermal retrocycloaddition of pyrrolidinofullerenes (retro-Prato reaction), *Chem.–Eur. J.*, 2008, **14**, 5198–5206, DOI: 10.1002/chem.200800096.

21 S. Osuna, M. Swart and M. Sola, Dispersion corrections essential for the study of chemical reactivity in fullerenes, *J. Phys. Chem. A*, 2011, **115**, 3491–3496, DOI: 10.1021/jp1091575.

22 N. M. Thong, *et al.*, Functionalization of fullerene via the Bingel reaction with alpha-chlorocarbanions: an ONIOM approach, *J. Mol. Model.*, 2016, **22**, 113, DOI: 10.1007/s00894-016-2981-5.

23 S. Grimme, S. Ehrlich and L. Goerigk, Effect of the damping function in dispersion corrected density functional theory, *J. Comput. Chem.*, 2011, **32**, 1456–1465.

24 C. F. Hsu, H. Peng, C. Basle, J. Travas-Sejdic and P. A. Kilmartin, $ABTS^{\bullet+}$ scavenging activity of polypyrrole, polyaniline and poly(3,4-ethylenedioxythiophene), *Polym. Int.*, 2011, **60**, 69–77, DOI: 10.1002/pi.2912.

25 M. Gizdavic-Nikolaidis, J. Travas-Sejdic, P. A. Kilmartin, G. A. Bowmaker and R. P. Cooney, Evaluation of antioxidant activity of aniline and polyaniline, *Curr. Appl. Phys.*, 2004, **4**, 343–346, DOI: 10.1016/j.cap.2003.11.044.

26 M. D. Tzirakis and M. Orfanopoulos, Radical reactions of fullerenes: from synthetic organic chemistry to materials science and biology, *Chem. Rev.*, 2013, **113**, 5262–5321, DOI: 10.1021/cr300475r.

27 A. D. Becke, Density-functional thermochemistry. III. The role of exact exchange, *J. Chem. Phys.*, 1993, **98**, 5648–5652, DOI: 10.1063/1.464913.

28 C. Lee, W. Yang and R. G. Parr, Development of the Colle-Salvetti correlation-energy formula into a functional of the electron density, *Phys. Rev. B: Condens. Matter Mater. Phys.*, 1988, **37**, 785–789, DOI: 10.1103/PhysRevB.37.785.

29 *Gaussian 09, Revision A.02*, Gaussian, Inc., Wallingford CT, 2009.

30 K. Hedberg, *et al.*, Bond lengths in free molecules of buckminsterfullerene, c60, from gas-phase electron diffraction, *Science*, 1991, **254**, 410–412, DOI: 10.1126/science.254.5030.410.

31 K. U. Ingold and D. A. Pratt, Advances in radical-trapping antioxidant chemistry in the 21st century: a kinetics and mechanisms perspective, *Chem. Rev.*, 2014, **114**, 9022–9046, DOI: 10.1021/cr500226n.

32 L. Echegoyen and L. E. Echegoyen, Electrochemistry of Fullerenes and Their Derivatives, *Acc. Chem. Res.*, 1998, **31**, 593–601, DOI: 10.1021/ar970138v.

33 A. Martinez, R. Vargas and A. Galano, What is important to prevent oxidative stress? A theoretical study on electron-transfer reactions between carotenoids and free radicals, *J. Phys. Chem. B*, 2009, **113**, 12113–12120, DOI: 10.1021/jp903958h.

34 W. Cai, Y. Chen, L. Xie, H. Zhang and C. Hou, Characterization and density functional theory study of the antioxidant activity of quercetin and its sugar-containing analogues, *Eur. Food Res. Technol.*, 2013, **238**, 121–128, DOI: 10.1007/s00217-013-2091-x.

35 J. J. Yin, *et al.*, The scavenging of reactive oxygen species and the potential for cell protection by functionalized fullerene materials, *Biomaterials*, 2009, **30**, 611–621, DOI: 10.1016/j.biomaterials.2008.09.061.